AGU PUBLICATIONS

Geophysical Research Letters

RESEARCH LETTER
10.1002/2016GL069140

**Key Points:**
- Shock-induced dropout drift echoes of >300 keV electrons at L∼6 are observed for the first time
- The dropout is localized at duskside according to the energy dispersion of the echoes
- Such dropout echoes are not caused by magnetopause shadowing

**Correspondence to:**
Q.-G. Zong,
qgzong@pku.edu.cn

**Citation:**
Hao, Y. X., et al. (2016), Electron dropout echoes induced by interplanetary shock: Van Allen Probes observations, *Geophys. Res. Lett.*, *43*, 5597–5605, doi:10.1002/2016GL069140.

Received 13 APR 2016
Accepted 10 MAY 2016
Accepted article online 16 MAY 2016
Published online 7 JUN 2016
Corrected 24 JUN 2016

This article was corrected on 24 JUN 2016. See the end of the full text for details.



# Electron dropout echoes induced by interplanetary shock: Van Allen Probes observations

**Y. X. Hao[1], Q.-G. Zong[1], X.-Z. Zhou[1], S. Y. Fu[1], R. Rankin[2], C.-J. Yuan[3], A. T. Y. Lui[4], H. E. Spence[5], J. B. Blake[6], D. N. Baker[7], and G. D. Reeves[8]**

[1]Institute of Space Physics and Applied Technology, Peking University, Beijing, China, [2]Department of Physics, University of Alberta, Edmonton, Alberta, Canada, [3]Institute of Geology and Geophysics, Chinese Academy of Sciences, Beijing, China, [4]Applied Physics Laboratory, Johns Hopkins University, Laurel, Maryland, [5]Department of Physics Institute for Earth, Oceans and Space, University of New Hampshire, Durham, New Hampshire, USA, [6]The Aerospace Corporation, Los Angeles, California, USA, [7]Space and Atmospheric Sciences Group, Los Alamos National Laboratory, Los Alamos, New Mexico, USA, [8]Laboratory for Atmospheric and Space Physics, University of Colorado, Boulder, Colorado, USA

**Abstract** On 23 November 2012, a sudden dropout of the relativistic electron flux was observed after an interplanetary shock arrival. The dropout peaks at ∼1 MeV and more than 80% of the electrons disappeared from the drift shell. Van Allen twin Probes observed a sharp electron flux dropout with clear energy dispersion signals. The repeating flux dropout and recovery signatures, or “dropout echoes”, constitute a new phenomenon referred to as a “drifting electron dropout” with a limited initial spatial range. The azimuthal range of the dropout is estimated to be on the duskside, from ∼1300 to 0100 LT. We conclude that the shock-induced electron dropout is not caused by the magnetopause shadowing. The dropout and consequent echoes suggest that the radial migration of relativistic electrons is induced by the strong dusk-dawn asymmetric interplanetary shock compression on the magnetosphere.

## 1. Introduction

The initial enhancement of energetic particle fluxes in the inner magnetosphere has been found to be closely related with substorm activities, and is therefore referred to as “substorm injections” [e.g. *Konradi*, 1967]. The drift echoes of such injected charged particles in the magnetosphere have long been discussed. *Lanzerotti et al.* [1967] examined the energy dependence of the period of observed electron flux oscillations and attributed periodic flux enhancement-recovery behavior to longitudinal drift of bunches of electrons. Drift echoes of energetic protons were also recognized [*Lanzerotti et al.*, 1971]. Utilizing the time delay relations of the drift motion, *Pfitzer and Winckler* [1969] determined that the source of substorm injected particles is localized near midnight.

*McIlwain* [1974] introduced the concept of “injection boundary” in order to explain the dispersion of injection signals. Further studies [e.g. *Konradi et al.*, 1975; *Mauk and Meng*, 1983] led to the model of a double-spiral shaped injection boundary with its deepest earthward penetration at the midnight sector. Only plasma tailward of this boundary will be suddenly energized during the initial injection. The injection is followed by energy- and species-dependent drift motion, which leads to dispersive or dispersionless initial injections, depending on the relative position between spacecraft and the boundary. Statistical study on dispersionless injections [e.g. *Lopez et al.*, 1990] and observations on subsequent drift echoes [e.g. *Friedel et al.*, 1996] show good quantitative agreement with their model.

An effective technique to remotely sense both the injection time and azimuthal location of the injection boundary was developed, and is based on tracing back the drifting particles according to their energy dispersion profile [*Reeves et al.*, 1990]. Backward tracing was also discussed in detail in their successive research [*Reeves et al.*, 1991]. An alternative method to estimate the western (eastern) edge of the electron (ion) injection region was also proposed, utilizing the information of the injection peak duration [*Reeves et al.*, 1992].

Most drift echoes discussed till now are injection echoes by default [*Vampola and Korth*, 1992]. Although single drifting electron holes associated with substorm injections have been studied by *Sergeev et al.* [1992], sharp energetic particle flux dropout and their echoes, showing repeating flux dropout-recovery time profile, have not yet been directly reported. In this study, we report such dropout of energetic electron flux and its drift echoes at the outer edge of the outer radiation belt. These echoes indicate localized electron flux

10.1002/2016GL069140

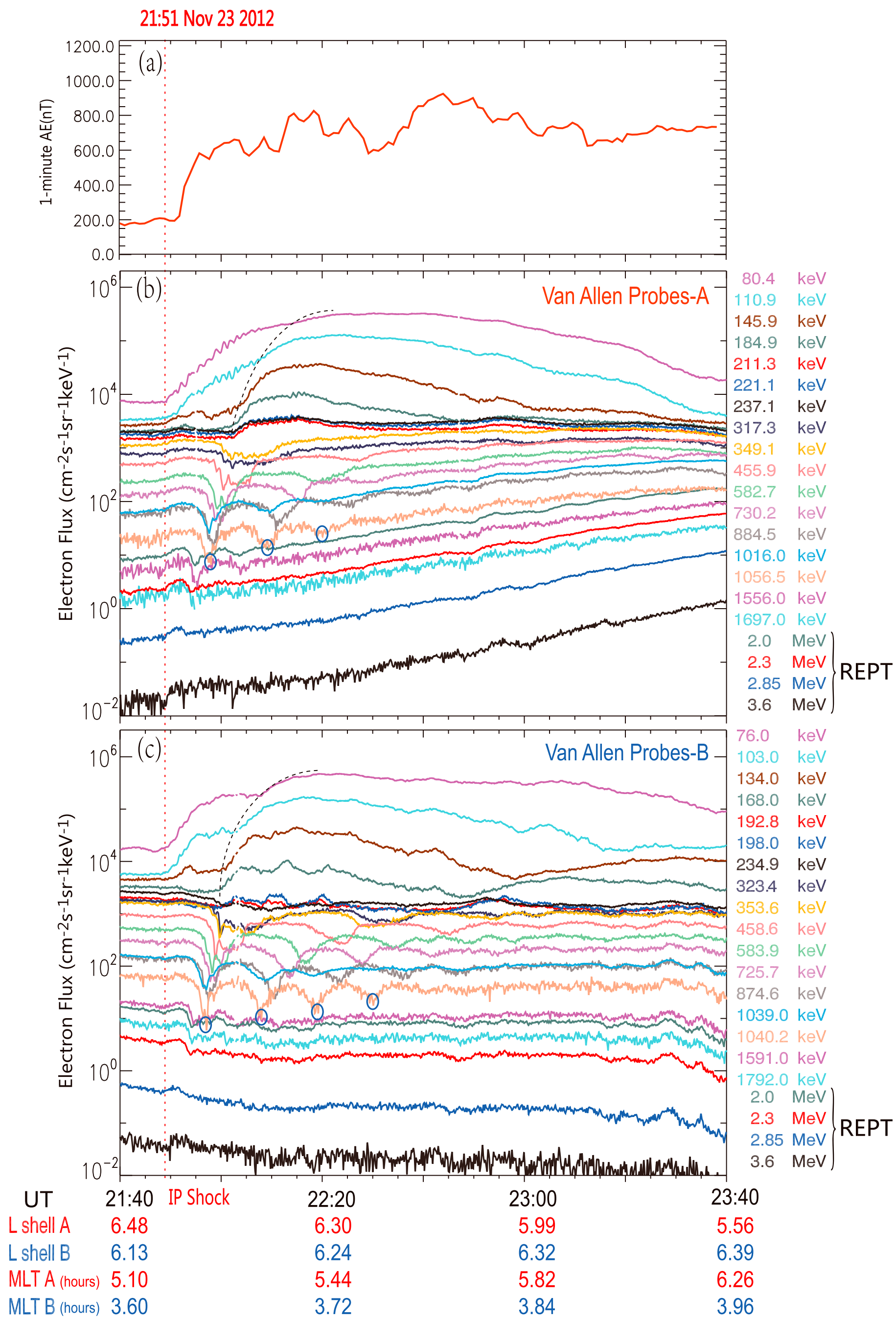


**Figure 1.** From top to bottom: The AE index, spin averaged energetic electron flux profile by MagEIS and REPT on Van Allen Probes A and B. Shock arrival time is marked with the red dashed line. Dropoout echoes are marked with blue circles.

dropout induced by an interplanetary shock. The azimuthal range, energy and pitch angle dependence of the dropout is investigated utilizing Magnetic Electron Ion Spectrometer (MagEIS) and Relativistic Electron Proton Telescope (REPT) [*Spence et al.*, 2013; *Blake et al.*, 2013; *Baker et al.*, 2013] measurements from the Van Allen Probes mission [*Mauk et al.*, 2014].

## 2. Observations

In this paper, we analyze the response of energetic and relativistic electrons in the terrestrial magnetosphere to an interplanetary shock occurring on 23 November, 2012 (suggested by SOHO Proton Monitor,

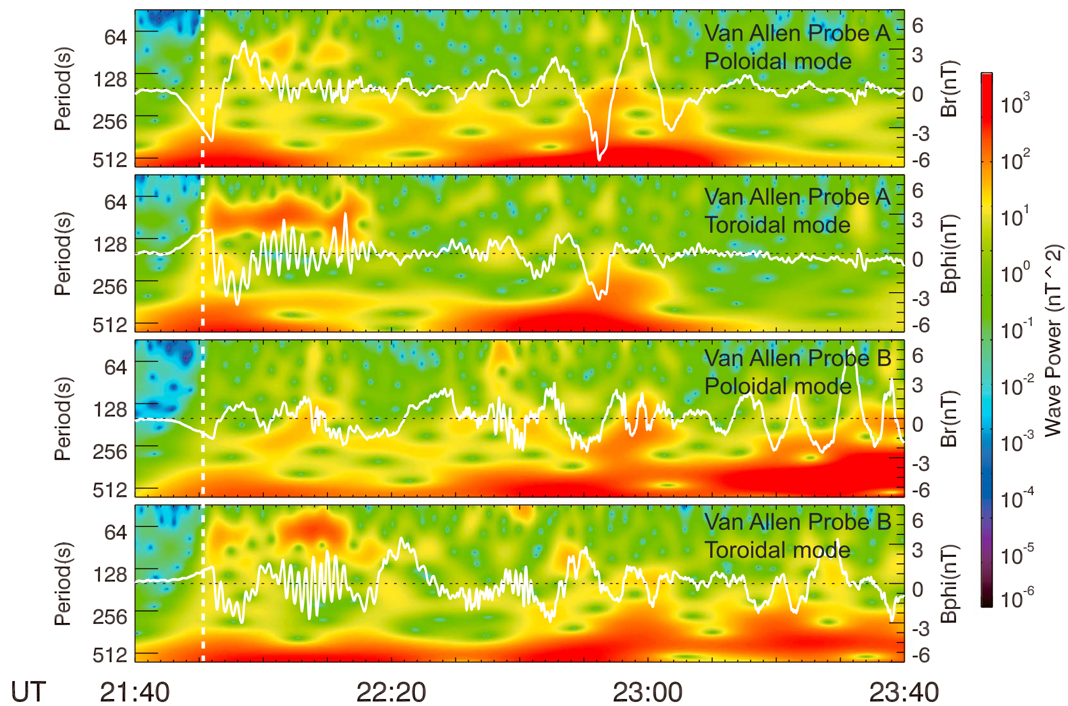


**Figure 2.** Pc 4-5 band ULF wave observations made by Van Allen Probes A and B. The magnetic field is projected onto a local mean-field-aligned (MFA) coordinate system [e.g. *Takahashi et al.*, 1990]. Magnetic field of poloidal and toroidal mode is plotted in white lines over their continuous wavelet power spectrum.

http://umtof.umd.edu/pm/FIGS.HTML). The Interplanetary Magnetic Field (IMF) precondition detected by WIND was around 3 nT southward (not shown). The shock arrival time is 2151 UT, as determined by GOES−15 magnetometer observations at the noon sector. After the shock arrival, the AE index increased by 450 nT (Figure 1), which can be recognized as a substorm-like event associated with interplanetary shock arrival, according to the previous statistical study of *Yue et al.* [2010]. They suggested that interplanetary shocks with a southward IMF precondition are most likely to induce substorm activities in the magnetosphere.

In the discussion that follows, data sets from MagEIS and REPT onboard the Van Allen Probes have been used to investigate the energetic and relativistic electrons in response to the interplanetary shock impact:

When the shock impinged on the magnetosphere, both Van Allen Probe spacecrafts were located at $L \sim 6$ with a small separation in the azimuthal direction: Probe A was at MLT~5 hours and Probe B was at MLT~4 hours. As shown in Figures 1b and 1c, when the shock impinged on the terrestrial magnetosphere, a flux enhancement of <300 keV electrons is observed by both spacecraft. As marked with dashed curves in Figures 1b and 1c, this flux enhancement shows significant energy dispersion: the fluxes of higher energy electrons are enhanced earlier. Such an energy dispersion indicates that the injection region is localized to the west of the satellites. The energetic electron injections(<300 keV), together with sudden enhanced AE index, suggest the occurrence of shock-induced substorm activity, which is consistent with previous event and statistical studies [e.g. *Yue et al.*, 2010].

Besides the injections, the fluxes of <300 keV electrons (e.g., 80.4 keV channel in Figure 1b) measured by Van Allen Probe A also show clear periodic oscillations. The periods of the flux oscillations are about 100 seconds, within Pc-4 band. Magnetic field pulsations of the same period also appear after the shock arrival. As shown in Figure 2, clear toroidal mode Pc-4 band ULF waves with a typical period near 100 seconds are observed by both Van Allen Probes A and B from 2151 UT to 2220 UT, while the poloidal mode ULF waves are relatively weaker during the same time interval. Hence the flux oscillations of <300 keV electron fluxes can be interpreted as a toroidal ULF wave modulation, which has been discussed by *Zong et al.* [2007].

However, when we examine the >300 keV electron flux variation carefully, their behavior distinctly differs from the lower energy channels. As can be seen in Figure 1, instead of dispersive injections, both spacecraft A and B observe a flux dropout in >300 keV channels a few minutes after the shock arrival. The fluxes recovers nearly

10.1002/2016GL069140

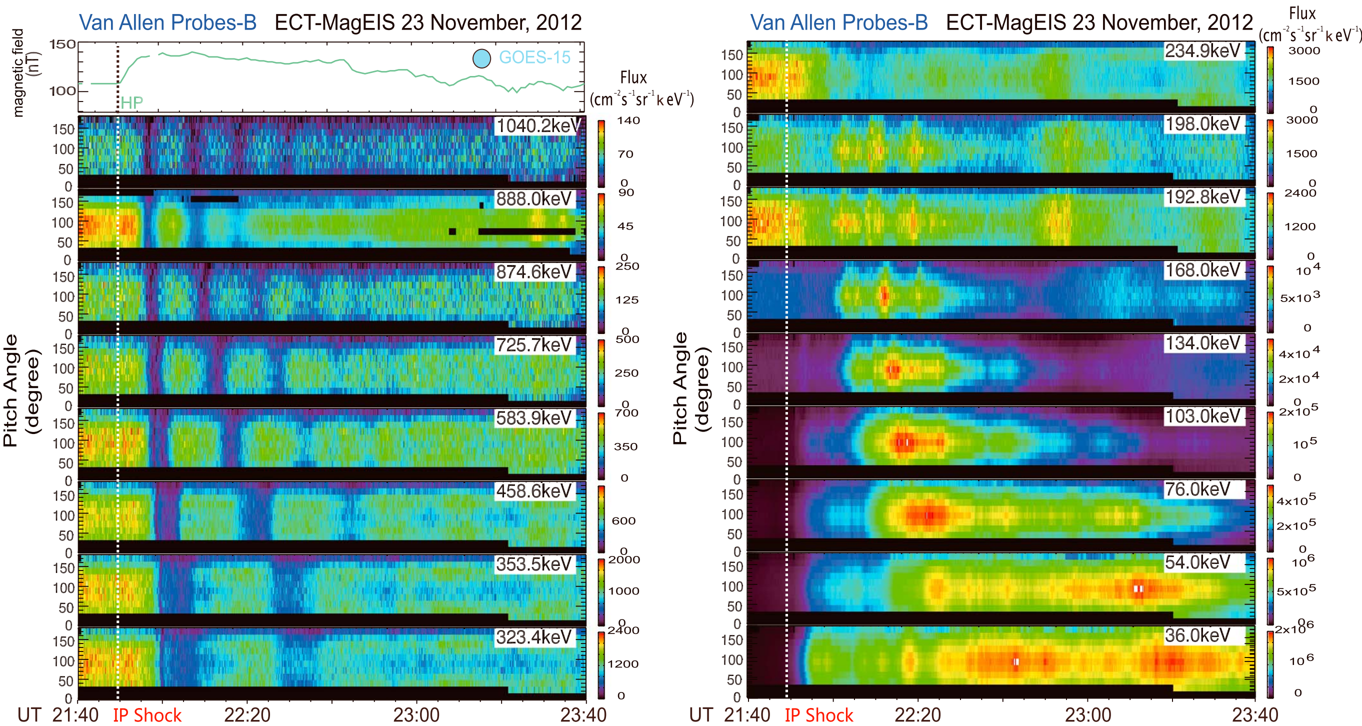


**Figure 3.** First Panel: Magnetic field perpendicular to the orbital plane of GOES 15 at noon sector. Other Panels: Pitch angle distribution evolution of the energetic electrons observed by MagEIS on Van Allen Probes B. Energy dispersion in both flux dropouts of 300-1000 keV electrons and injections of lower energy channels are clear.

to their initial level within 20 minutes after the dropout. For instance, time interval between 50% dropout and 50% recovery is around 240 seconds for the flux of 1040.2 keV channel measured by spacecraft B. The upper bound energy of the electron flux dropout is around 2.3 MeV. This flux dropout-recovery signal repeats more than 4 times for channels covering 350-1050 keV, with periods approximately consistent with their drift periods. We suggest that the repeating flux dropout-recovery signals in these channels are drift echoes of an initial dropout. As a counterpart of the well-documented injection echoes [e.g. *Reeves et al.*, 1990], we define these echoes as "dropout echoes".

To further investigate the initial dropouts and their echoes, we plot the pitch angle evolution profile of 30–1000 keV electrons in Figure 3. Higher energy and time resolution MagEIS data enable us to look closely into these "dropout echoes". The dropouts can be seen clearly for electrons in the >300 keV channels. Note that the flux dropout occurs at all pitch angles, although for each energy channel the dropouts appear slightly earlier at 90° pitch angle than at other pitch angles. Also, the flux dropouts are significantly energy-dispersed: the fluxes of higher energy electrons dropout earlier.

Electron flux dropouts are also observed by GOES 13,14 and 15 satellites, as shown in Figure 4. As marked with blue arrows in Figure 4, sharp flux dropouts are observed in 275 keV, 475 keV and > 0.8 MeV channels by GOES 13 and GOES 14 within 10 minutes after the shock arrival (21:51 to 22:01, the gray shaded area in Figure 4). Such dropout is not observed by GOES 15 during this time interval. Following the initial dropout, after 22:01 UT, GOES 13 and 14 both observed another minimum of electron flux at the > 0.8 MeV channel. Flux dropouts of >0.8 MeV and >2.0 MeV electrons are also observed by GOES 15 after 22:01 as marked with red arrows in Figure 4. We suggest that those flux dropout signals marked with red arrows during 22:01 to 22:14 (green shaded area in Figure 4) are drift echoes, similar with what Van Allen Probes have observed.

## 3. Interpretation and Discussion

### 3.1. Energy Dependence and Location of the Dropout Echoes

In order to understand the interplanetary shock-induced sudden flux dropout and the consequent "dropout echoes", we examine quantitatively their associated energy dispersion and pitch angle dependence.

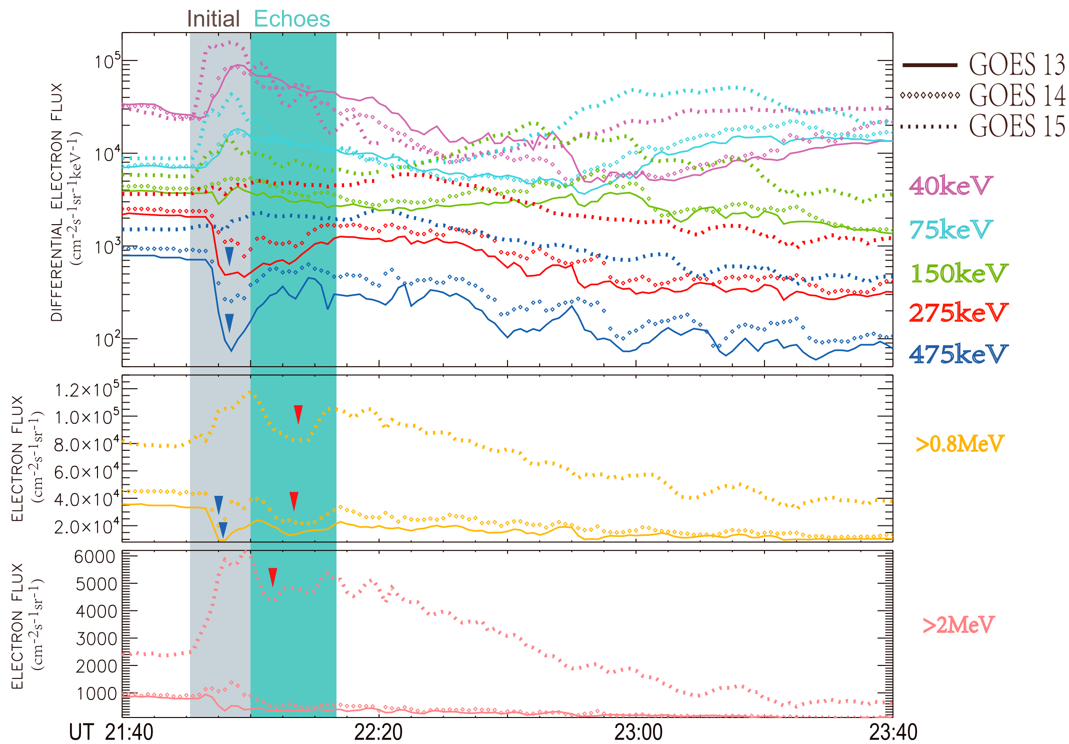


**Figure 4.** Electron flux measured by GOES 13, 14 and 15 (solid lines for GOES 13, diamonds for GOES 14 and dashed lines for GOES 15). Dropouts in gray shaded area (2151 UT to 2201 UT) and green shaded area (2201 UT to 2214 UT) are marked with blue and red arrows respectively, representing initial dropouts and their echoes.

The energy and pitch-angle dependence of the dropout is shown in Figure 5. In Figure 5a, the strongest dropout appears at 500 keV – 1 MeV in which the electron fluxes drop to 10% – 20% of the pre-event level. The pitch angle distribution (PAD) of the representative 725 keV electrons is presented in Figure 5b. Before the shock arrival, the electrons show mostly a pancake distribution, whereas during the dropout event, a roughly isotropic PAD appears below the previous pancake PAD. This evolution of the PAD indicates that: 1. Dropout of electrons happens at all pitch angles, 2. Electrons of 90° pitch angle experience strongest flux dropout.

As shown in Figure 3, the electron fluxes of higher energy and pitch angle closer to 90°, in other words, higher drift speed, drop earlier. Such dispersion suggests an original dropout region azimuthally to the west of Van Allen Probes. Analogous to the substorm injection process, the remote sensing technique of *Reeves et al.* [1990] can be applied to determine the location and starting time of the sudden electron flux dropout:

As shown in Figures 6a and 6b, the observed dropout onset time (east edge of the "dropout cloud") and dropout recovery time (west edge) are defined by the points when the fluxes drop (recover) by 50%. The intersections of both satellite observation indicate that the dropout sector is localized counterclockwise from *LT*~13 hours to *LT* ~01 hours. This result indicates that the shock-induced dropout is impulsive and is a localized phenomenon rather than a global one. Since the dropout echoes do not originate from dawn sector, the Pc-4 ULF waves observed there by Van Allen twin Probes (see Figure 2) may not be considered directly as their driving force.

As shown in Figure 4, electron flux dropouts are also observed by the GOES 13 and 14 satellites but not by GOES 15. This can be explained as that GOES 13 and 14 are located in the dropout area, while GOES 15 is near the boundary of the area, which accounts well for the spontaneous, dispersionless flux dropout observed by GOES 13 and 14. For the dropout recovery phase, we can also obtain the western edge of the dropout through backward tracing according to the observed dropout duration [similar to *Reeves et al.*, 1990, 1992].

The same technique can be applied to the injected energetic electron and proton populations associated with the interplanetary shock impact as well. The injection profiles of <300 keV electrons and 150 – 500 keV protons from Van Allen Probes B can be utilized to determine the eastern and western edge of the injection. It can be seen clearly that the injection happens from *LT* ~ 19 hours to *LT* ~ 03 hours at nightside while the dropout

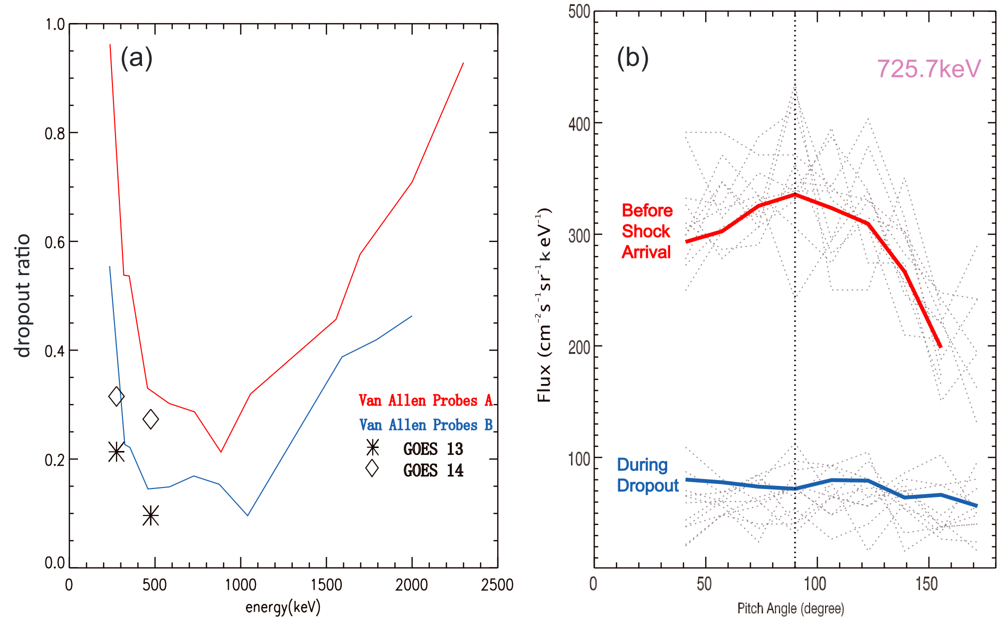


**Figure 5.** (a): The ratio between the minimum electron flux during the initial dropout and the flux before the shock arrival. (b): 100-second average of the Unidirectional Differential Electron Flux (FEDU) data from MagEIS of Van Allen Probes B. The red line represents the pitch angle distribution of 725.7 keV electrons before the shock arrival while the blue line represents the distribution during the initial dropout. Original data before being averaged is plotted in gray lines.

happens from $LT \sim 13$ hours to $LT \sim 01$ hours at duskside. All of the results discussed above are summarized in Figure 6. The observations suggest that the electron dropouts and injections occur at different regions, possibly due to different mechanisms for dropouts and injections.

### 3.2. On the Dropout Echoes

As interpreted in the last subsection, shock induced electron flux dropout peaks at 500 keV – 1 MeV, and shows a 90° pitch angle dominance. Both remote sensing and in-situ observations suggest that the dropout is localized at duskside (0100 – 1300 LT). These results provide us clues to understand the dropout mechanism:

Previous studies have revealed that, during geomagnetic storms [e.g. *Ukhorskiy et al.*, 2006; *Turner et al.*, 2012; *Degeling et al.*, 2013], an inward motion of the dayside magnetopause in response to the shock passage can pump electrons out immediately and efficiently from the magnetosphere, known as "magnetopause shadowing". *Wilken et al.* [1986] have also reported dispersive dropout of proton fluxes related to magnetopause shadowing. Accompanied with sequent ULF wave driven radial diffusion, magnetopause shadowing can lead to outer belt particle flux dropouts even during a nonstorm period with continuously positive SYM-H index and northward IMF [*Katsavrias et al.*, 2015]. However, the electron flux dropout caused by magnetopause shadowing should be localized near the noon sector, which contradicts our observation: both GOES 15 in-situ observation and Van Allen Probes remote sensing suggest that the dropout region is located at 1300 LT to 0100 LT, rather than at the noon sector. The magnetopause standoff distance is estimated to move from 10.1 $R_E$ to 8.3 $R_E$ according to the change of the solar wind dynamic pressure ($P_{dyn}$ from 1.2 nPa to 4 nPa). The change of the magnetopause standoff distance is not likely to produce the dropout and consequent "dropout echoes" at the vicinity of geosynchronous orbit (at around 6.6 $R_E$) as observed by Van Allen Probes A & B. On the other hand, the fluxes of energetic ions observed by Van Allen Probes A & B do not show evidence of dropouts (plots are not shown here). Thus, a simple magnetopause block of the particle drift path is unlikely to result in the observations shown in this paper. In addition, the time scale for ULF-wave-driven radial diffusion to cause significant dropout is in the order of several hours. Whereas our observations suggest that the dropout induced by the shock is rather limited on temporal scale (e.g. 240 seconds for 1040.2 keV electrons). Thus, the MeV electron flux dropout echoes may be caused by a different mechanism rather than radial diffusion driven by ULF waves following the initial magnetopause shadowing.

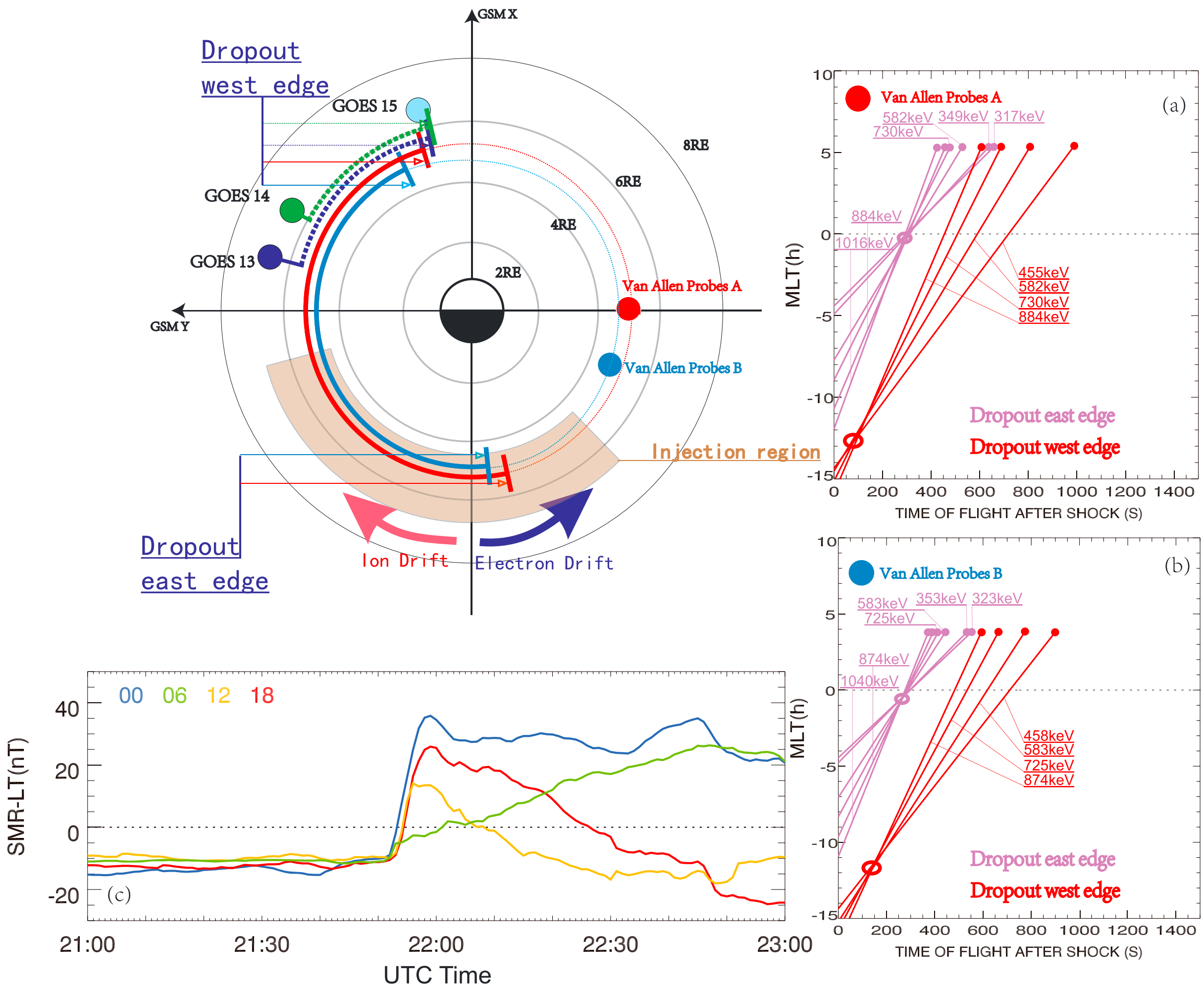

**Figure 6.** (a and b): dots show the time when dropout front and back are observed by each MagEIS energy channel on Van Allen Probes A and B and spacecraft positions then, the slopes of the solid line varies according to the drift speed of electrons with 90° pitch angle in an idealized terrestrial dipole field. Thus, here the intersections of the lines indicate the boundary and time of the dropout. Center: spacecraft positions are projected into Geocentric Solar Magnetospheric Coordinate System (GSM) x-y plane. Red and blue solid lines indicate the dropout region determined with Van Allen Probes A and B observations according to Figures 6a and 6b. Deep blue and green dashed lines mark the western edge of the dropout region according to GOES-13 and 14 electron flux measurements. Shock induced substorm injection of lower energy particles is marked in brown, eastern edge according to Van Allen Probes A Energetic particle, Composition, and Thermal plasma (ECT)-MagEIS electron measurement and the western edge according to Van Allen Probes B ECT-MagEIS proton measurement.
(c): SuperMAG observation of partial ring current indices of four sectors (SMR-LT).

In other studies conducted by *Li et al.* [1998, 2003], simulations reproduced flux decrease of MeV electrons accompanying substorm injection. In these simulations, both the injection of lower energy electrons and the decrease of MeV electrons are driven by a transient westward electric field associated with the substorm dipolarization. Different flux variations between low and high energy electrons are interpreted as a lack of source population at larger radial distances. Observational studies [*Sergeev et al.*, 1992] also show drifting holes of >300 keV electrons associated with substorm injection near magnetic midnight. Although observations have shown that particles with energy less than 300 keV are injected by interplanetary shock-triggered substorm from the midnight sector, the dropouts with energy great than 300 keV are mostly originated in the duskside magnetosphere. In addition, GOES 13 and 14 are located out of the western edge of the injection region. Nevertheless, GOES 13 and 14 do observe the dispersionless dropouts (see Figure 4). Therefore, the substorm dipolarization may not be applied to explain the observations presented in this paper.

Another process of energetic particle loss via tail lobe entry has been discussed by *Moldwin et al.* [1995]; *Fennell et al.* [1997]. They show that complete dropouts of energetic electrons in the inner magnetosphere can be caused by electrons escaping into the tail lobe (open field lines). As shown in Figure 4, electron flux (>150 keV) dropouts are observed by the GOES 13 and 14 satellites, however, electron fluxes between 45 keV and 150 keV are enhanced rather than dropped out after the shock arrival. This indicates that both the GOES 13 and 14 satellites are not located on open field lines (lobe field lines). Therefore, the electron dropout echoes observed in this paper are most likely not due to energetic electron escaping via open field lines.

Partial ring current indices (SMR-LT) based on the SuperMAG collaboration can be utilized to study global geomagnetic response to interplanetary shocks. Rotated to a local magnetic coordinate, with baseline including the diurnal variations, yearly trend and residual offset subtracted [*Gjerloev*, 2012], ground-based magnetometer measurements are utilized to calculate an average "H" component for four sectors separately. According to definition made by *Newell and Gjerloev* [2012], SMR-00 covers 2100-0300 LT thus stands for the midnight sector, and so on. As we can see from Figure 6 (left bottom), SMR-LT show strong asymmetric response produced by the interplanetary shock with dawn enhanced the least, midnight/dusk the most. Following the interplanetary shock arrival, the midnight sector SMR-LT index shows similar response to those in the noon and dusk sectors. Consequently, the radial motion of electrons in the magnetosphere will be caused by the sudden strong distortion of geomagnetic field with the field compressed more at duskside than at dawnside. Thus, the observed electron flux dropout and the consequent echoes may result from the radially-inward energetic electron migration caused by the strong asymmetry following the interplanetary shock compression on the magnetosphere.

## 4. Summary

In this paper, we have presented evidence of electron flux dropouts with energy up to 2.0 MeV. The dropouts are accompanied by drift echoes subsequent to an interplanetary shock impinging on the magnetosphere. Dispersive energetic dropouts are located between at MLT ~0400 and 0500 at $L \sim 6$ on 23 November, 2012 as observed by Van Allen twin Probes. Main results are summarized as followings:

1. Only high energy electron profiles show clear dropout while low energy electrons show an injection related to substorm behaviour. The crossover energy is around 300 keV. The dropout of electron flux peaks at 500 keV – 1 MeV, with a dropout ratio 0.1 – 0.2.
2. The dropouts observed initially are clearly dispersive, which along with the following drift echoes indicates a localized rather than a global behaviour. Calculations based on the dispersion of the dropouts indicate that the dropout region is located in the 1300 – 0100 LT sector, not collocated with the substorm injection region (mid-night sector).
3. The dropout of electron population occurs at all pitch angle but peaks at 90° pitch angle.

In conclusion, the observed shock-induced electron dropout is probably not caused by magnetopause shadowing or lobe entry. The observed electron flux dropout and its consequent echoes can be explained as sudden inward radial migration of energetic electrons driven by the shock-induced dusk-dawn asymmetric compression of the magnetosphere. Statistical studies and test-particle simulations are still needed for further understanding of the energy, pitch angle and local time dependence of such shock-induced dropouts.

**Acknowledgments**
This work was supported by National Natural Science Foundation of China (41421003 and Major Project of Chinese National Programs for Fundamental Research and Development (2012CB825603). We acknowledge Space Physics Data Facility, Goddard Space Flight Center (http://cdaweb.gsfc.nasa.gov/) for providing all data in this article. Thanks Ying Liu and Jie Ren for helpful discussion.

## References

Baker, D., et al. (2013), The relativistic electron-proton telescope (rept) instrument on board the Radiation Belt Storm Probes (RBSP) spacecraft: Characterization of Earth's radiation belt high-energy particle populations, *Space Sci. Rev.*, *179*(1 – 4), 337 – 381, doi:10.1007/s11214-012-9950-9.

Baker, D. N., R. D. Belian, P. R. Higbie, and E. W. Hones (1979), High-energy magnetospheric protons and their dependence on geomagnetic and interplanetary conditions, *J. Geophys. Res.*, *84*(A12), 7138 – 7154, doi:10.1029/JA084iA12p07138.

Blake, J., et al. (2013), The Magnetic Electron Ion Spectrometer (MAGEIS) instruments aboard the Radiation Belt Storm Probes (RBSP) spacecraft, *Space Sci. Rev.*, 1 – 39.

Degeling, A. W., R. Rankin, K. Murphy, and I. J. Rae (2013), Magnetospheric convection and magnetopause shadowing effects in ULF wave-driven energetic electron transport, *J. Geophys. Res. Space Physics*, *118*, 2919 – 2927, doi:10.1002/jgra.50219.

Fennell, J., J. Blake, J. Roeder, R. Sheldon, and H. E. Spence (1997), Tail lobe and open field line region entries at mid to high latitudes, *Adv. Space Res.*, *20*(3), 431 – 435.

Friedel, R. H. W., A. Korth, and G. Kremser (1996), Substorm onset observed by CRRES: Determination of energetic source region, *J. Geophys. Res.*, *101*, 13,137 – 13,154.

Gjerloev, J. (2012), The supermag data processing technique, *J. Geophys. Res.*, *117*, A09213, doi:10.1029/2012JA017683.

Katsavrias, C., I. Daglis, D. Turner, I. Sandberg, C. Papadimitriou, M. Georgiou, and G. Balasis (2015), Nonstorm loss of relativistic electrons in the outer radiation belt, *Geophys. Res. Lett.*, *42*, 10,521 – 10,530, doi:10.1002/2015GL066773.

Konradi, A. (1967), Proton events in the magnetosphere associated with magnetic bays, *J. Geophys. Res.*, *72*(15), 3829 – 3841.

Konradi, A., C. L. Semar, and T. A. Fritz (1975), Sunstorm-injected protons and electrons and the injection boundary model, *J. Geophys. Res.*, *80*, 543 – 552.

Lanzerotti, L., C. Roberts, and W. Brown (1967), Temporal variations in the electron flux at synchronous altitudes, *J. Geophys. Res.*, *72*(23), 5893 – 5902.

Lanzerotti, L. J., C. G. Maclennan, and M. F. Robbins (1971), Proton drift echoes in the magnetosphere, *J. Geophys. Res.*, *76*, doi:10.1029/JA076i001p00259.
Li, X., et al. (1998), Energetic electron injections into the inner magnetosphere during the Jan. 10-11, 1997 magnetic storm, *Geophys. Res. Lett.*, *25*, 2561–2564.
Li, X. L., et al. (2003), Energetic particle injections in the inner magnetosphere as a response to an interplanetary shock, *J. Atmos. Sol. Terr. Phys.*, *65*, 233–244.
Lopez, R. E., D. G. Sibeck, R. W. McEntire, and S. M. Krimigis (1990), The energetic ion substorm injection boundary, *J. Geophys. Res.*, *95*, 109–117.
Mauk, B., and C.-I. Meng (1983), Characterization of geostationary particle signatures based on the 'injection boundary' model, *J. Geophys. Res.*, *88*(A4), 3055–3071.
Mauk, B., N. J. Fox, S. Kanekal, R. Kessel, D. Sibeck, and A. Ukhorskiy (2014), Science objectives and rationale for the radiation belt storm probes mission, *Space Sci. Rev.*, *179*, 2–27, doi:10.1007/s11214-012-9908-y.
McIlwain, C. E. (1974), Substorm injection boundaries, in *Magnetospheric Physics*, edited by B. M. McCormac, pp. 143–154, D. Reidel, Hingham, Mass.
Moldwin, M. B., M. F. Thomsen, S. J. Bame, D. J. McComas, J. Birn, G. D. Reeves, R. Nemzek, and R. D. Belian (1995), Flux dropouts of plasma and energetic particles at geosynchronous orbit during large geomagnetic storms: Entry into the lobes, *J. Geophys. Res.*, *100*(A5), 8031–8043.
Newell, P., and J. Gjerloev (2012), Supermag-based partial ring current indices, *J. Geophys. Res.*, *117*, A05215, doi:10.1029/2012JA017586.
Pfitzer, K., and J. Winckler (1969), Intensity correlations and substorm electron drift effects in the outer radiation belt measured with the ogo 3 and ats 1 satellites, *J. Geophys. Res.*, *74*(21), 5005–5018.
Reeves, G., R. Belian, and T. Fritz (1991), Numerical tracing of energetic particle drift in a model magnetosphere, *J. Geophys. Res.*, *96*(A8), 13,997–14,008.
Reeves, G. D., T. A. Fritz, T. E. Cayton, and R. D. Belian (1990), Multi-satellite measurements of substorm injection region, *Geophys. Res. Lett.*, *17*, 2015–2018.
Reeves, G. D., G. Kettmann, T. A. Fritz, and R. D. Belian (1992), Further investigation of the CDAW 7 substorm using geosynchronous particle data: Multiple injections and their implications, *J. Geophys. Res.*, *97*, 6417–6428.
Sergeev, V., T. Bösinger, R. Belian, G. Reeves, and T. Cayton (1992), Drifting holes in the energetic electron flux at geosynchronous orbit following substorm onset, *J. Geophys. Res.*, *97*(A5), 6541–6548.
Spence, H. E., et al. (2013), Science goals and overview of the Radiation Belt Storm Probes (RBSP) Energetic Particle, Composition, and Thermal Plasma (ECT) suite on NASA's van allen probes mission, *Space Sci. Rev.*, *179*, 311–336, doi:10.1007/s11214-013-7420007-5.
Takahashi, K., R. W. McEntire, A. T. Y. Lui, and T. A. Potemra (1990), Ion flux oscillations associated with a radially polarized transverse Pc 5 magnetic pulsation, *J. Geophys. Res.*, *95*, 3717–3731.
Turner, D. L., Y. Shprits, M. Hartinger, and V. Angelopoulos (2012), Explaining sudden losses of outer radiation belt electrons during geomagnetic storms, *Nat. Phys.*, *8*(3), 208–212.
Ukhorskiy, A., B. Anderson, P. Brandt, and N. Tsyganenko (2006), Storm time evolution of the outer radiation belt: Transport and losses, *J. Geophys. Res.*, *111*, A11S03, doi:10.1029/2006JA011690.
Vampola, A. L., and A. Korth (1992), Eletron drift echos in the inner magnetosphere, *Geophys. Res. Lett.*, *19*, 625–628.
Wilken, B., D. N. Baker, P. R. Higbie, T. A. Fritz, W. P. Olson, and K. A. Pfitzer (1986), Magnetospheric configuration and energetic particle effects associated with a SSC: A case study of the CDAW event on March 22, 1979, *J. Geophys. Res.*, *91*, 1459–1473.
Yue, C., et al. (2010), Geomagnetic activities triggered by interplanetary shocks, *J. Geophys. Res.*, *115*, A00I05, doi:10.1029/2010JA015356.
Zong, Q.-G., et al. (2007), Ultralow frequency modulation of energetic particles in the dayside magnetosphere, *Geophys. Res. Lett.*, *34*, L12105, doi:10.1029/2007GL029915.

## Erratum

In the originally published version of this article, the first key point included a typographical error in a mathematical value: the value should have been >300 keV electrons not <300 keV electrons. This error has been corrected, and this version may be considered the authoritative version of record.